

4

DTIC FILE COPY

Contract N00014-86-K-0842

Final Report

AD-A205 944

## EXPERIMENTAL OBSERVATION OF CRISIS INDUCED INTERMITTENCY

W. L. Ditto, R. Cawley, C. Grebogi<sup>+</sup>, E. Ott<sup>+</sup>, S. Rauseo,  
H. T. Savage, R. Segnan<sup>\*</sup>, M. Spano, J.A. Yorke<sup>+</sup>

Naval Surface Warfare Center, Silver Spring, MD 20903-5000

<sup>+</sup>University of Maryland, College Park, MD 20742

<sup>\*</sup>The American University, Washington, DC 20016

### ABSTRACT

The first reported observation of crisis induced intermittency (sudden chaotic attractor widening with its characteristic temporal behavior as a system parameter is varied) has been observed in a parametrically driven gravitationally buckled amorphous ribbon experiment. The experimental results are in excellent agreement with the predictions made by Grebogi, et. al. for the temporal behavior of nonlinear flows and maps near a crisis.

See next page

This document has been approved  
for public release and sale in  
distribution is unlimited.

DTIC  
ELECTE  
S 27 MAR 1989 D  
9  
E

89 3 16 038

A gravitationally buckled amorphous ribbon driven parametrically by a time varying magnetic field (Figure 1(a)) has been observed to exhibit sudden chaotic attractor widening (and consequent intermittency) as the drive frequency is varied. The temporal behavior of this system shows excellent agreement with the characteristic temporal behavior termed crisis induced intermittency by Grebogi, Ott, Romeiras and Yorke<sup>1</sup> in their study of intermittency in nonlinear flows and maps.

We have observed that a crisis occurs in our system as the driving frequency  $f$  decreases through a critical value  $f_c$ . For  $f < f_c$  the chaotic motion typically remains for a long time in a region near its initial buckled state called the core attractor. A crisis then occurs in which the motion suddenly bursts into a more remote region made available by the crisis, stays there briefly and returns to the core attractor. Experimentally a burst consists of the ribbon starting from the initially buckled configuration, passing through the vertical unstable equilibrium position, buckling on the opposite side for a period of time and then returning to the side of the initial buckling.

→ The ribbon that is used in the experiment is a member of a new class of amorphous ferromagnetic materials that has been discovered<sup>2</sup> to exhibit very large, rapid, reversible changes of Young's modulus  $E(H)$  with the application of a magnetic field (Fig. 1(b)). Using this large change in modulus, Savage and Adler have reported<sup>3</sup> how a vertical, amorphous ribbon, clamped at the bottom and free at the top, can be made to buckle under its own weight and subsequently unbuckle by increasing a magnetic field from zero to magnetic saturation. The process is as follows: The critical height  $h_c$  at which a vertical column will buckle under its own weight depends on its stiffness, i.e.,  $h_c$  is proportional to  $[E(H)]^{1/3}$ . In the experiment  $E(H)$  can be changed by changing the value

— (KR) —

of the vertical field  $H$ , thus changing the value of  $h_c$  below and above the height  $h$  of the ribbon.

In the one-dimensional theory<sup>2</sup> used to describe the experiment, a magnetostrictive "Hooke's law" for the material was shown to be  $e = T/E_0 - (3\lambda/2)(M/M_s)^2$ , where  $\lambda = 3.0 \times 10^{-5}$  is the magnetostriction constant,  $E_0 = 2 \times 10^{12}$  J/m<sup>3</sup> is Young's modulus at infinite field,  $M_s = 1.7$  T is the saturation magnetic moment and  $e$ ,  $T$  and  $M$  are the longitudinal (vertical) strain, stress, and magnetic moment respectively. In this theory a finite stress-strain expression was shown to be<sup>2</sup>

$$T = \sum a_n(H) (e - e_0)^n$$

where  $e_0$  is the strain at zero stress. The coefficients  $a_n$  are completely determined from other experiments<sup>2</sup>. The coefficient  $a_1$  in the series is  $E(H)$  and is shown by the smooth curve in Fig. 1a. The measurement of  $E(H)$  in resonance experiments is also shown. Values of the magnetic field that cause buckling were found to be in good agreement with predictions based on the values of the eigenvalues (which depend upon  $E(H)$ ) of the linearized operator describing the experiment.<sup>2</sup>

Since the  $a_n$  are all functions of  $H$ , we can magnetically change the elastic nonlinearity by changing  $H$ . The ribbon can be made elastically linear with  $M = 0$  or at magnetic saturation ( $M = M_s$ , which occurs at large  $H$ ). The buckling of the ribbon is governed by a quasilinear system of partial differential equations<sup>2</sup> and is parametrically driven by changing  $H$ . A restoring torque proportional to  $M H \sin \theta$ , where  $\theta$  is the angle between the ribbon and the field, is also present but can be shown to be quite small.



By _____	
Distribution/ _____	
Availability Codes	
Dist	Avail and/or Special
A-1	

The experiment consists of a  $\text{Fe}_{81}\text{B}_{13.5}\text{Si}_{3.5}\text{C}_2$  amorphous ferromagnetic ribbon,  $25\mu\text{m}$  thick, 3 mm wide, and .1 m long clamped at the base to yield a 650 mm free vertical height. A pair of Helmholtz coils and an HP3325A frequency synthesizer were used to produce a bias (constant) vertical magnetic field  $H_0$  and an alternating vertical magnetic field component with amplitude  $H_{ac}$  and driving frequency  $f$ , i.e.,  $H = H_0 + H_{ac} \cos(2\pi ft)$ . An MTI 1000 Fonic sensor, centered 6mm from the clamped base of the ribbon, was used to obtain a time series of the horizontal displacement that was stored at a rate of 42.7 samples/sec on a PDP/11. Runs of 100,000 points (39 min. duration) were obtained for many driving frequencies. The ribbon was started from an initially buckled configuration by adjusting  $h$  to a value slightly larger than  $h_c$  at  $H = 0$ .

A phase space study was performed and an attractor was reconstructed from the time series by embedding the time series data points labeled  $P_1, P_2, P_3, \dots$  in a  $d$ -dimensional phase space using the usual technique of a delay coordinate embedding and forming the  $d$ -tuple  $(P_i, P_{i+n}, P_{i+2n}, \dots, P_{i+(d-1)n})$  for the points  $P_i$  for the time series<sup>4</sup>. The delay  $n$  selected was the common choice of the first minimum of the autocorrelation function of the data and was determined to be 15 data points (yielding a delay of .35 sec). The attractors, for frequencies before and after the crisis are shown in Fig. 2a and Fig. 2b respectively. The time between bursts  $t_b$  was measured as the length of time the orbit spends in the core attractor. Values of  $t_b$  exhibited a Poisson distribution ( Fig. 3 ) if times shorter than a minimum time,  $t_0 = 11.5$  sec, were not used in the analysis. The value of  $t_0$  reflects the time required for the orbit to settle onto the core attractor after a burst has ended. The value of  $t_0$  is independent of the frequency providing it is still sufficiently close to the critical frequency. The characteristic time  $\tau$ , averaged over the time series of 39 min, for bursts lasting longer than  $t_0$ , has been measured at many

frequencies close to  $f_c$ . In Fig. 4 the characteristic time clearly exhibits the power law  $\tau = (f_c - f)^{-\gamma}$  as predicted in Ref. 3. The value of  $\gamma$ , the critical exponent, is found to be  $.827 \pm .05$ .

Poincaré sections have been obtained for the attractor by constructing the 3 dimensional delay coordinate embedding  $(X_1, X_2, X_3)$  where  $X_1 = P_i$ ,  $X_2 = P_{i+15}$ ,  $X_3 = P_{i+30}$  for the points  $P_i$  of the time series and defining the section to be the plane  $S$  defined by

$$S = \{ (X_1, X_3) \mid X_1 = X_2 \text{ and } \dot{X}_1 > \dot{X}_2 \} .$$

Fig. 5a and Fig. 5b exhibit sections before and after the crisis respectively. The additional regions visited in Fig. 5b exhibit few points as indicated by the short periods of time spent bursting. It is important to note the existence of an unstable period 9 orbit A:  $A_1 \rightarrow A_2 \rightarrow A_3 \rightarrow \dots \rightarrow A_9 \rightarrow A_1 \rightarrow \dots$  and an unstable period 3 orbit B:  $B_1 \rightarrow B_2 \rightarrow B_3 \rightarrow B_1 \rightarrow \dots$ . Analysis of the sections and time series indicated that for  $f = f_c$  the unstable manifold for the period 9 orbit A becomes tangent to the stable manifold of the period 3 orbit B, which is on the boundary of the attractor. The orbit then initiates a burst by shooting out along the unstable manifold of B. The crisis is heteroclinic because a burst was always preceded by the characteristic period 9 to period 3 sequence.

By examining the preiterates and postiterates of the period 9 orbit A the eigenvalues  $\alpha_1$  (expanding direction) and  $\alpha_2$  (contracting direction) for A were calculated to be ?? and ?? respectively. For a heteroclinic crisis the critical exponent  $\gamma$  is <sup>3</sup>,  $\gamma = 1/2 + \ln(|\alpha_1|) / |\ln|\alpha_2||$ , yielding the value  $\gamma = .9 \pm .1$ , which is in good agreement with the experimental value determined previously.

We can conclude that our experimental results provide evidence of crisis induced intermittency in amorphous ferromagnetic ribbons and the validity of the method proposed by Grebogi et. al. for determining the critical exponents for the temporal dependence of the intermittency from an experimental time series.

We acknowlege the valuable discussions and help of Marilyn Wun-Fogle, Guan Hsu and Stuart Antman and thank Howard Lieberman of Allied corporation for the sample. Additionally W. L. Ditto would like to thank Dr. C. E. G. Przirembel and the ONT/ASEE Post-Doctoral program.

### REFERENCES

1. Celso Grebogi, Edward Ott, Filipe Romeiras, and James A. Yorke, Phys. Rev. **A36**, 5365 (1987).
2. H. T. Savage, Charles Adler, Journal of Magnetism and Magnetic Materials, **58**, 320 (1986).
3. H. T. Savage, M. L. Spano, J. Appl. Phys. **53**(11), 8092 (1982).
4. D. Ruelle, F. Takens, Commun. Math. Phys. **20**, 167 (1971).

### FIGURE CAPTIONS

- Fig. 1 (a) Experimental arrangement for the buckling ribbon.  
(b) Normalized Young' modulus,  $E(H)/E_0$  vs magnetic field  $H$  in transverse-field annealed, amorphous  $\text{Fe}_{81}\text{B}_{13.5}\text{S}_{3.5}\text{C}_2$ .
- Fig. 2 Attractors (a)  $f = .835 \text{ Hz} > f_c$  (before crisis) and (b)  $f = .830 \text{ Hz} < f_c$  (after crisis).
- Fig. 3 Poisson distribution of bursting times  $t_b$  at a driving frequency of .830 Hz. The "non-Poisson" first 11.5 sec is the time for the orbit to settle on the core attractor.
- Fig. 4.  $\text{Ln}(\tau)$  vs  $\text{Ln}(f - f_c)$ .  $\tau$  is the average time between bursts and  $f$  is the driving frequency.
- Fig 5. Poincaré sections (a)  $f = .835 \text{ Hz} > f_c$  (before crisis) and (b)  $f = .830 \text{ Hz} < f_c$  (after crisis). The  $A_n$  (period 9 unstable orbit points) are illustrated in (a) and are similarly located in (b). The  $B_n$  (period 3 unstable orbit points) lie on the boundary of the core attractor and appear only in (b).

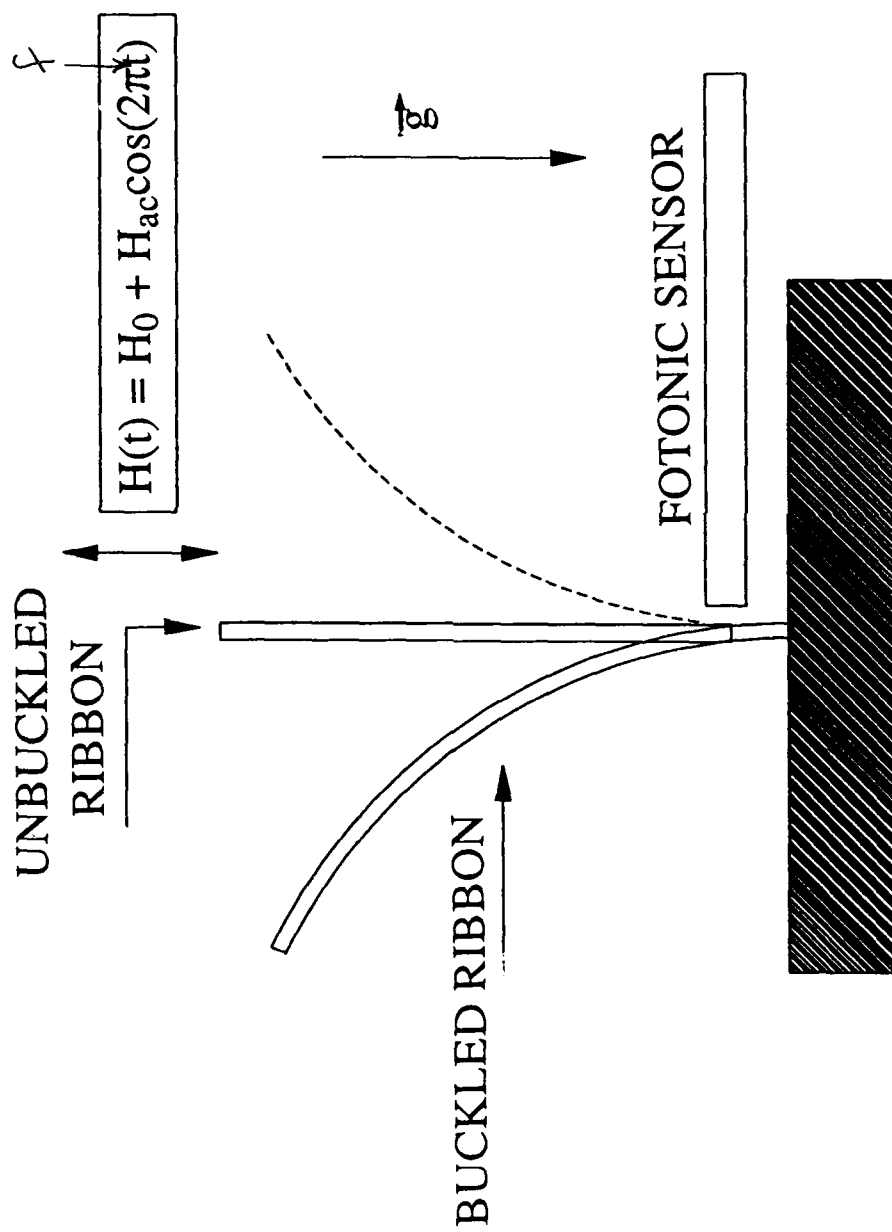


Figure 1(a)



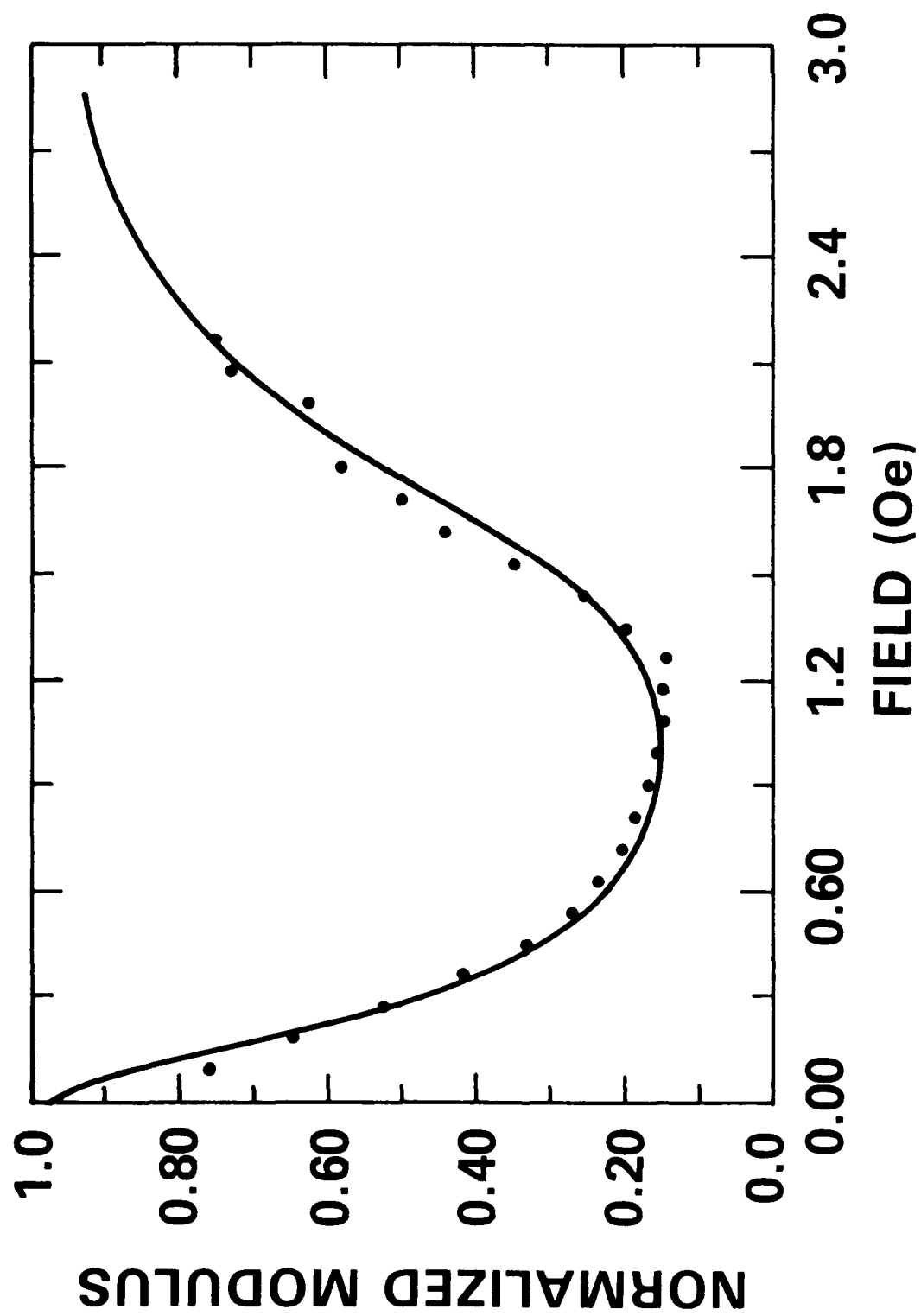


FIGURE 1(b)

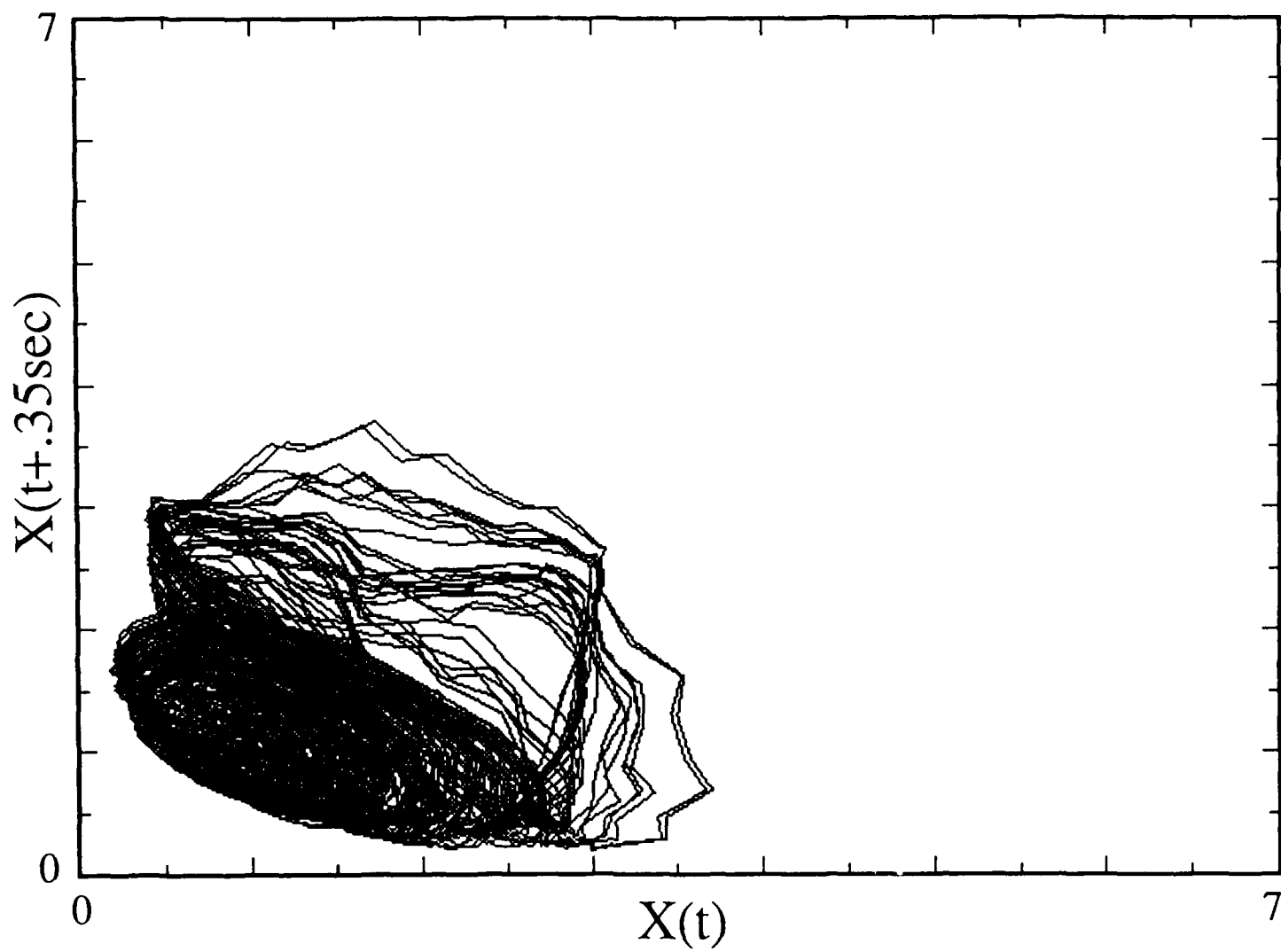


Figure 2 (a)

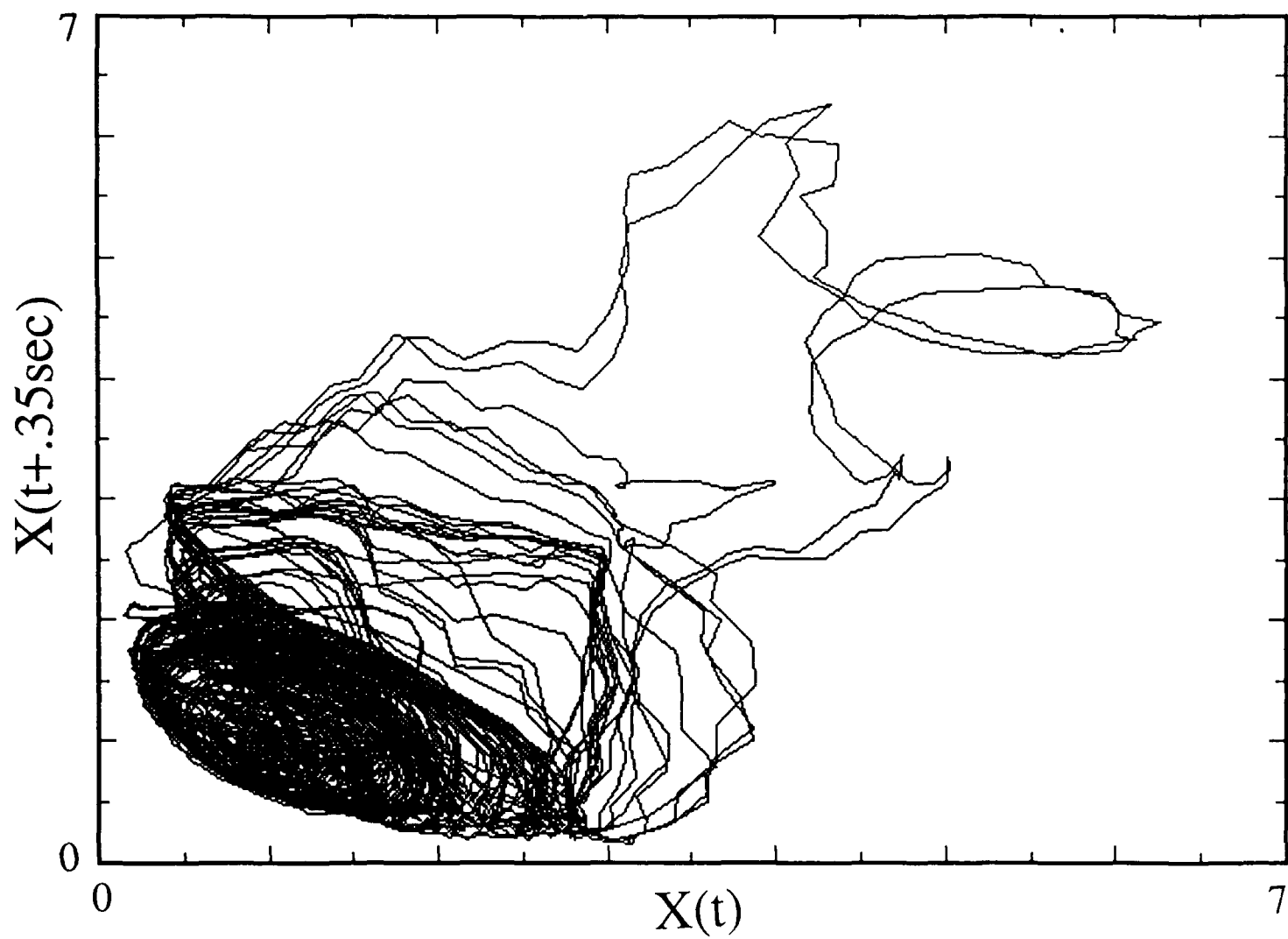


Figure 2(b)

$\bar{\tau}$  vs  $|f-f_c|$ , for  $f_c = 0.8344$  Hz

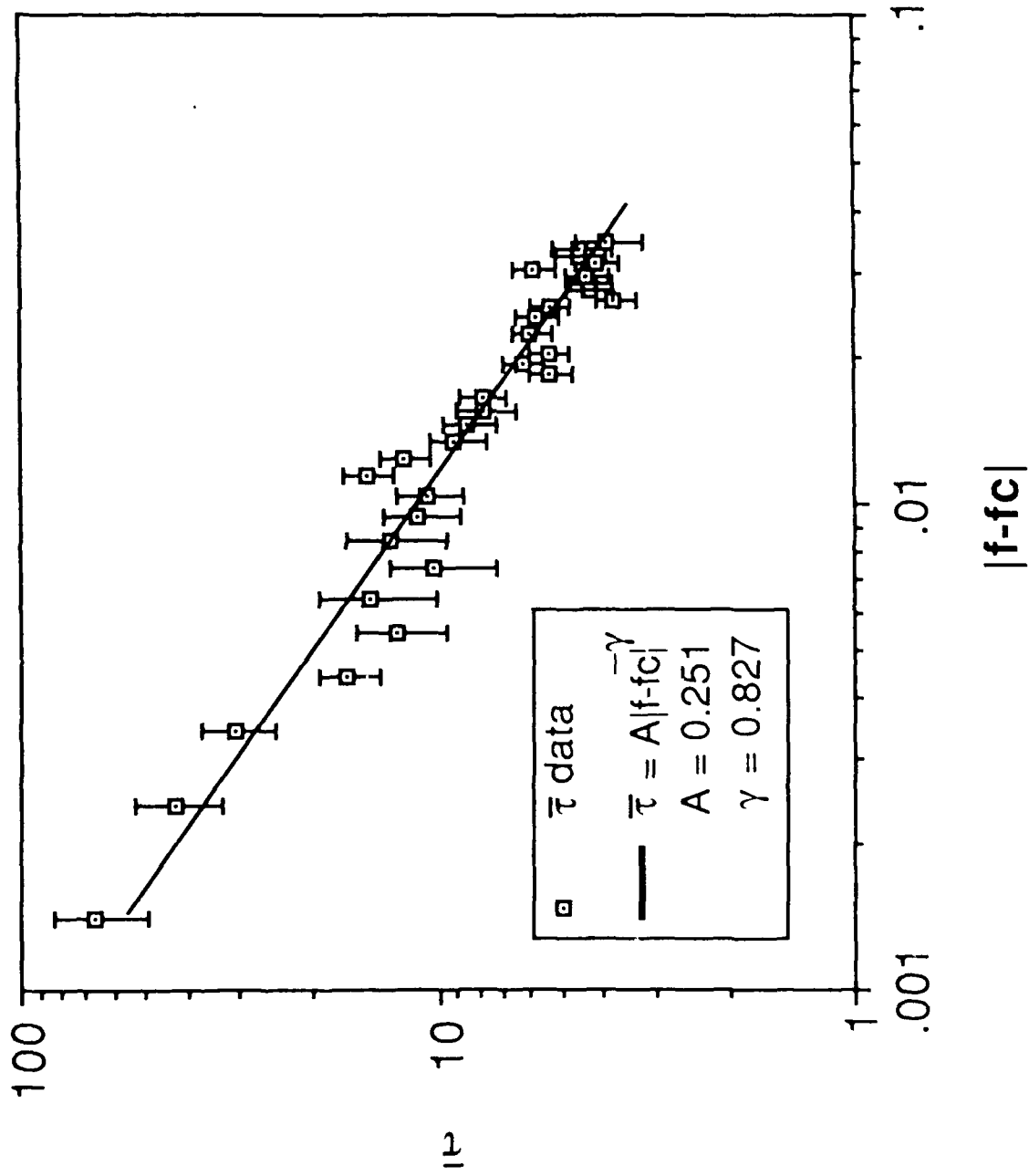


Figure 4

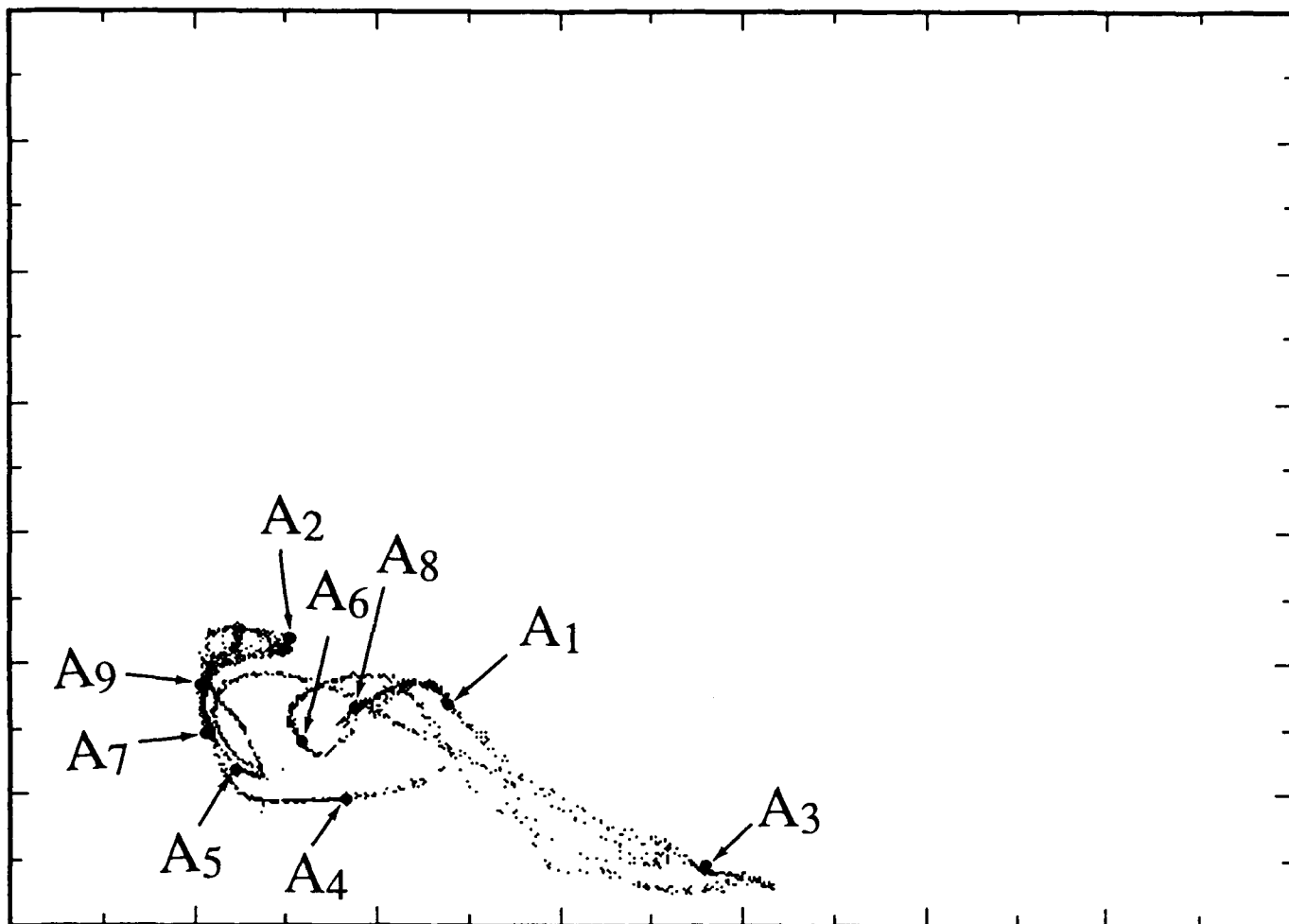


Figure 5(a)

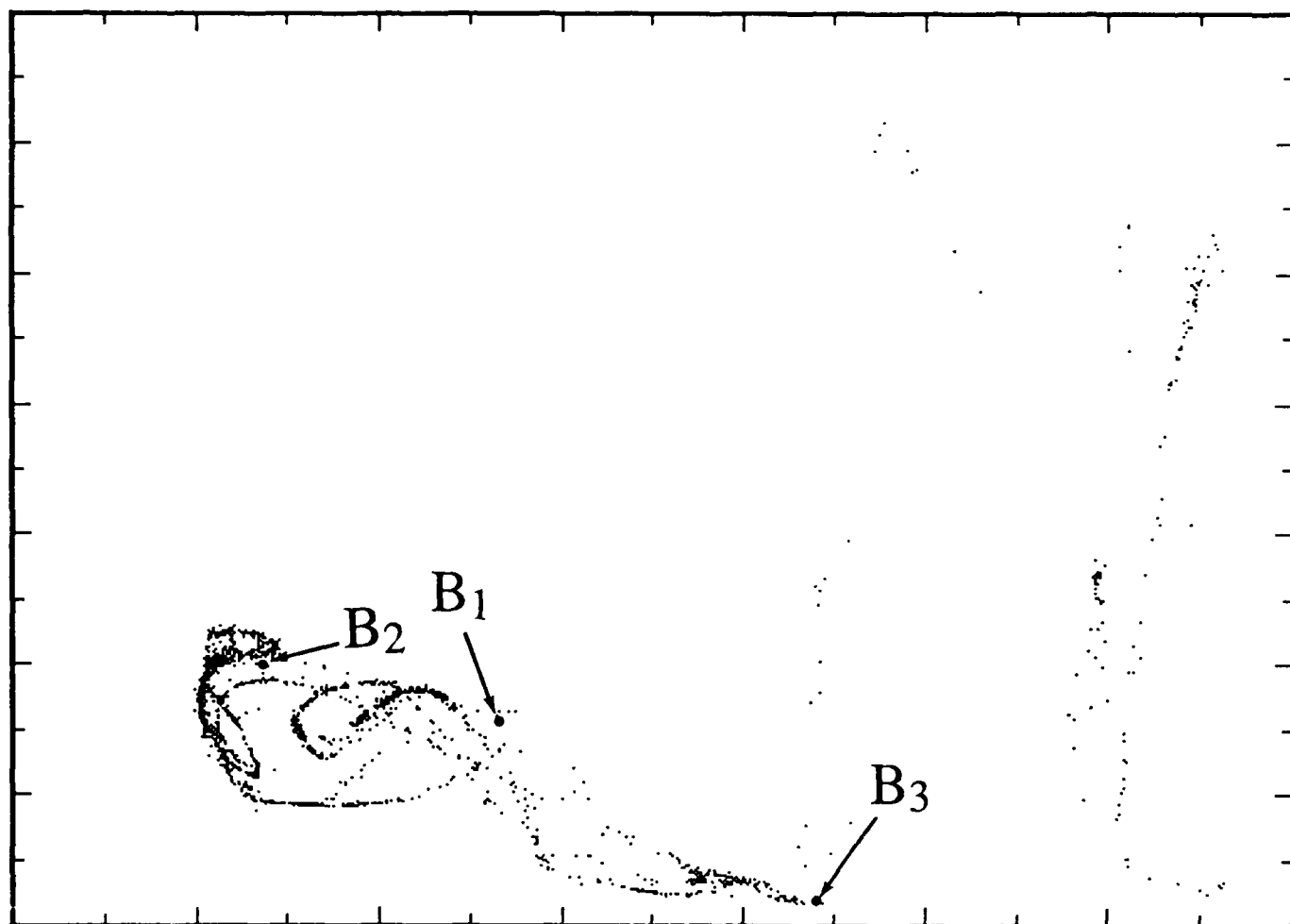


Figure 5 (b)